Egyptian Journal of Radiology and Nuclear Medicine

RESEARCH

Open Access

Effect of hepatic fat fraction on major hepatocellular carcinoma features at magnetic resonance imaging

Mohamed Fouad Osman[1], Ahmed Ramadan Mohammed[1,3], Amr Abd Elfattah Hassan Gadalla[1], Mohammed Mahmoud Abdelhamid Ali[2] and Bahaa Eldin Mahmoud[1*]

Abstract

Background Hepatocellular carcinoma (HCC) is the fifth most frequent cancer on the world. Fat accumulation within hepatocytes is known as hepatic steatosis. In recent years, research has found that people with non-alcoholic fatty liver disease have a higher chance of developing HCC. The LI-RADS® (Liver Imaging Reporting and Data System) was created to facilitate consistent reporting of imaging findings in patients at risk of HCC. The aim of this study was to see how hepatic fat fraction affects the LI-RADS major HCC features on magnetic resonance imaging (MRI).

Results All HCCs (92/92; 100%) showed arterial phase hyperenhancement (APHE); however, a significant association between hepatic steatosis and late APHE was found. Encapsulation was observed in 51 HCC (55.4%); in hepatic steatosis patients 17 HCC (37.8%) displayed enhancing capsule in delayed phase of the study, compared to 34 HCC (72.3%) in non-steatotic patients. The HCC size ranged from 11 to 200 mm (Mean 42.2 ± 51.8 mm) in the hepatic steatosis group; however, in patients with negative hepatic steatosis the size ranged from 13 to 205 (Mean 62.9 ± 54.5 mm).

Conclusions Hepatic steatosis had a significant association with absent enhancing capsule, late arterial enhancement, as well as a lesion size less than 50 mm. "Fat sparing in solid mass" and "non-enhancing capsule" ancillary features had a significant association with hepatic steatosis, while "mild–moderate T2 hyperintensity" and "fat in mass, more than adjacent liver" ancillary features had a significant association with absent hepatic steatosis.

Keywords Carcinoma, Hepatocellular, Fatty liver, LI-RADS, Magnetic resonance imaging

Background

Hepatic steatosis, also known as simple steatosis, is a reversible disease in which big vacuoles of triglyceride fat deposit in hepatocytes. In spite of its many causes, fatty liver is regarded as a singular disease which affects people all over the world who drink too much alcohol or are obese. It is difficult to tell the difference between alcoholic fatty liver disease (AFLD) and non-alcoholic fatty liver disease (NAFLD) because both have microvesicular and macrovesicular fatty changes at differing stages [1]. The gold standard for liver histological tests is a liver biopsy; however, it is an aggressive technique that is hard to repeat. Furthermore, this technique only obtains a small portion of the liver, which may result in sampling bias [2]. An increased number of researches have found moderate-to-strong associations between MR measurements and steatosis measurements in biopsy histological Sections [3].

Hepatocellular carcinoma (HCC) is the fifth most common cancer worldwide. Cirrhosis is a key risk

*Correspondence:
Bahaa Eldin Mahmoud
bahaa.mahmoud@kasralainy.edu.eg
[1] Department of Radiology, Faculty of Medicine, Cairo University, Giza, Egypt
[2] Department of Radiology, Students' Hospital, Cairo University, Cairo, Egypt
[3] Department of Hepatology and Endemic Medicine, Faculty of Medicine, Cairo university, Giza, Egypt

factor for the development of HCC, especially cirrhosis caused by chronic viral hepatitis and alcoholic cirrhosis [4]. According to recent studies, patients with NAFLD have an increased chance of developing HCC. Because HCC can occur in NAFLD without hepatic fibrosis or cirrhosis, it is unclear who should be evaluated for HCC when the traditional risk indicators are not present [5]. In oncology, assessing the therapeutic approach normally necessitates tissue sampling before the diagnosis of malignancy. Hepatocellular carcinoma (HCC), on the other hand, is an exception since imaging can be employed to determine a noninvasive diagnosis in these high-risk populations [6]. Hepatocellular carcinoma (HCC) has been well described in terms of its imaging characteristics in individuals with liver cirrhosis. On contrast-enhanced imaging, hyperenhancement during the arterial phase and a subsequent washout during the enhancement phase serve as the primary diagnostic indicators. When both of these characteristics are met, the diagnosis of HCC can be made with high levels of certainty, eliminating the need for a second confirming tumor biopsy. But these standards were not explicitly created for HCCs that arise in people with non-alcoholic steatohepatitis; instead, they were designed for HCCs in people with liver cirrhosis [7]. The LI-RADS was employed to enhance standardization and agreement in the accuracy, interpretation, and reporting of liver CT and MRI in patients at high risk for developing HCC. The LI-RADS classifies the nodules found on computed tomography (CT) or MRI into 5 categories from I to V: definitively benign, possibly benign, intermediate likelihood of being HCC, probably HCC, and definitively HCC [8].

The aim of this study was to see how hepatic fat fraction affects the LI-RADS major HCC features on MRI.

Methods

Patient selection

Between January 2020 and December 2020, a retrospective search was conducted to find all patients with HCC who underwent a magnetic resonance imaging (MRI) of the liver at the radiology department of our institution. Inclusion criteria included: (1) MRI of the liver included at least dynamic contrast-enhanced series and in- and opposed phase sequence and (2) hepatic focal lesion with MRI characteristics consistent with HCC. The first search resulted in a total of 125 patients. We excluded six individuals because they did not have in- and opposed phase imaging, and 27 patients had hepatic focal lesions that were not definitive hepatocellular carcinoma (LIRADS-M). A total of 92 cases with MRI characteristics consistent with HCC (LIRADS V) who had a liver MRI scan were eventually included in the research. The LI-RADS major HCC features were used to make the HCC diagnosis. The local ethical and institutional review boards gave their approval to this study. The institutional review board waived the necessity for written informed consent because of the retrospective methodology of the study.

MRI protocol

All patients underwent dynamic MRI of the liver using Philips 1.5 Tesla MRI scanner (Achieva). The gradient strength of the magnet was 45 mT/m, with a maximum gradient slope of 200 T/m/s. The following sequences (illustrated in Table 1) were obtained in all of the included studies: T2-W turbo spin echo (TSE) with fat suppression, ultra-fast spin echo (UFSE), single-shot turbo spin echo (SSH-TSE), unenhanced in-phase and out-of-phase T1-WI, and fat-suppressed 3D volumetric interpolated breath hold gradient-echo sequences before and after intravenous gadolinium chelate injection. The images were taken with the patients in a supine position. To

Table 1 MR imaging parameters

Variable Plane	T2 TSE Transverse	T1 in-phase Transverse	T1 out-of-phase Transverse	T2 UFSE Transverse and coronal	T1 3D THRIVE Transverse
Repetition time (ms)	1000	6.41–110	6.41–110	1000–1200	3.90–4.23
Echo time (ms)	88–121	2.56–4.77	1.28–2.39	89–95	1.48–2.03
Flip angle (°)	180	9–10	9–10	150	9–14
Fat suppression	Spectral	No	No	No	Spectral
Slice thickness (mm)	4.5–5	3–7.5	3–7.5	4.5–6	2.2
Intersection gap (mm)	0	0–1	0–1	0–1	0
Number of slices	24	24–80	24–80	19–24	72–120
Matrix size	256–320 × 256–384	320–352 × 182	320–352 × 182	256 × 198	320–384 × 234–240
Number of signal averages	1	1	1	1	1
Acquisition time (second)	150–320	19–28	19–28	24–26	17–23

achieve perfect registration between related pictures, in-phase and out-of-phase sequences were obtained using a dual echo technique. A dynamic series using 3 dimensions fat-sat T1-W gradient echo sequence (THRIVE, i.e., T1 high-resolution isotropic volume examination) was performed, and it consisted of precontrast images followed by 4 post-contrast series after intravenous administration of gadopentetate dimeglumine (MAGNEVIST®) at a dose of 0.1-mmol/kilogram. The study performed at 19–21 s intervals, encompassing early and late arterial phases, and portal phase. After that, 5-min delayed phase imaging is performed. With parallel acquisition (GRAPPA or controlled aliasing in parallel imaging resulting in greater acceleration factor [CAIPIRINHA]), a partial Fourier reconstruction (6/8) was employed, with an acceleration factor of 2 or 4. Fat suppression was achieved using the spectral selective attenuated inversion recovery (SPAIR) method. The 3D THRIVE acquisitions had done at the end of expiration while in suspended respiration.

MR image analysis

Multireader MRI review

Using a standardized form, two radiologists with experience in abdominal radiology independently assessed HCC features and characteristics of hepatic parenchyma using the available Picture archiving and communication system (PACS); one radiologist had 10 years of experience in abdominal radiology, and the other radiologist had 7 years of experience at the time of the study. The two radiologists were not given data about the patients to reduce review bias. Consensus was used to establish an agreement. A standard data collecting form was used to tabulate qualitative and quantitative information for all patients. Any available previous studies were reviewed for follow-up. HCC features evaluated according to LI-RADS v2018 included: major HCC features: (non-rim APHE, non-peripheral contrast washout, enhancing tumor capsule, size, threshold growth), ancillary features favoring malignancy: (corona enhancement, subthreshold growth, mild–moderate T2 hyperintensity, restricted diffusion, fat sparing in solid mass), ancillary features favoring HCC: nodule-in-nodule architecture, blood products in mass, non-enhancing tumor capsule, mosaic architecture, fat in mass more than adjacent liver. In the case of lesions with suspiciously high T1 signal, digital subtraction was utilized to evaluate post-contrast images. A peripheral enhancing ring on portal venous or delayed phases was characterized as a tumor capsule. Readers assess for enhancing "capsule" in the portal venous and delayed phases of the study. The radiologists used calipers in the axial plane to estimate tumor size obtained during the portal phase.

Hepatic cirrhosis

The radiologists looked at hepatic morphology for MRI abnormalities that could indicate liver cirrhosis. Surface irregularity, left lobe hypertrophy, caudate lobe hypertrophy, right lobe atrophy and widened inter-lobar fissure, as well as 2ry signs of portal hypertension (PHTN) such as enlarged spleen, ascites, and porto-systemic collaterals, were used to grade cirrhotic hepatic features.

Fat signal fraction (FS%) calculation

Another observer determined the hepatic fat signal fraction, on the in- and opposite phase pictures. In the posterior right hepatic lobe a region of interest (ROI) was applied at a single position, while avoiding tumor bearing areas, large vascular structures, artifact, or partial volume effects. In all cases, the ROIs were 1 cm in size. The formula: Fat fraction = [(SIP-SOP)/2*SIP)] was used to compute the hepatic FS fraction, where SIP stands for mean signal on in-phase images and SOP stands for mean signal on opposite phase images. Hepatic steatosis grades: (none (< 5%), mild (5–< 15%), moderate (15 – < 30%), and severe (≥ 30%)) [9, 10].

We categorize patients into two groups: (1) HCC with hepatic steatosis group: if there is MR evidence of hepatic steatosis (Hepatic FS % ≥ 5%). (2) HCC with no hepatic steatosis group: no MR evidence of hepatic steatosis (Hepatic FS % < 5%).

Statistical analysis

The Statistical Package of Social Science Software application, version 25, was used to enter data and do statistical analysis (IBM SPSS Statistics for Windows, Version 25.0. Armonk, NY: IBM Corp.). For quantitative data, mean and standard deviation were used, whereas for qualitative variables, frequency and percentage were used. The chi-square or Fisher's exact tests were used to compare groups on qualitative factors, whereas the Mann–Whitney test was used to compare groups on quantitative variables. To evaluate the relationship between distinct ordinal or quantitative variables, Spearman correlation coefficients were computed. Statistical significance was defined as a *P* value of less than or equal to 0.05.

Results

A total of 92 patients ranging in age from 15 to 80 years old were involved in the study (Mean ± SD = 60 ± 9.6), 72 were males representing 78.3% of the total number of patients, and 20 were females representing 21.7% of the total number of patients.

The hepatic fat fraction ranged from 0 to 41.7 (Mean ± SD = 5.8 ± 7.2) in all patients. In patients with

positive hepatic steatosis the hepatic fat fraction ranged from 5.1 to 41.7 (Mean ± SD = 10.6 ± 6.7). In patients with negative hepatic steatosis the hepatic fat fraction ranged from 0 to 4.8 (Mean ± SD = 0.8 ± 1.4).

We classified hepatic steatosis into the following grades: Hepatic steatosis grades: (none (< 5%), mild (5–< 15%), moderate (15 –< 30%), and severe (≥ 30%)) (Table 2).

Clinical and pathologic findings

The clinicopathological characteristics of all patients were presented in Table 3.

Comparison between positive and negative hepatic steatosis patients according to the presence of major HCC features (Fig. 1) (Table 4):

On arterial phase imaging, all HCC (92/92; 100%) displayed hyperenhancement when compared to the surrounding hepatic parenchyma. However, it was found that late APHE had a significant association with hepatic steatosis with *p* value 0.000.

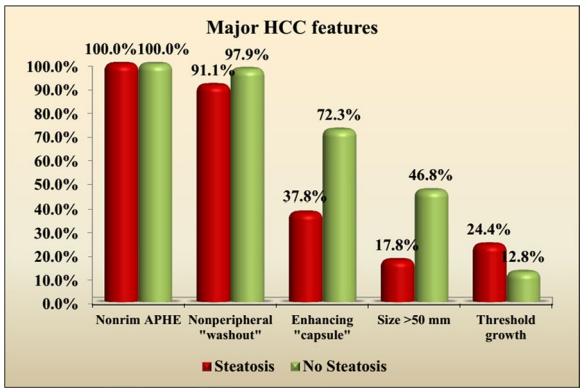

Fig. 1 A graph showing the difference between positive and negative hepatic steatosis patients according to the presence of major HCC features

Table 2 Hepatic steatosis grades

None	Fatty liver 45 (48.9%)		
	Mild	Moderate	Severe
47 (51.1%)	34 (37.0%)	9 (9.8%)	2 (2.2%)

On portal phase and/or delayed phase imaging, 87 HCC (94.6%) showed contrast washout. In the patients with positive hepatic steatosis 41 HCC (91.1%) displayed delayed contrast washout, compared to 46 HCC (97.9%) in negative hepatic steatosis patients. The result was not statistically significant with *P* value 0.175.

The enhancing capsule feature was observed in 51 HCC (55.4%) (Fig. 2). In the patients with positive hepatic

Table 3 Clinical and pathological data

	Fatty liver (*n* = 45)	Non-fatty liver (*n* = 47)	*p* value
Age (year), mean ± SD, range	60.7 ± 8.3 (40–80)	59.4 ± 10.6 (15–77)	0.931
Sex			
Male	38 (84.4)	34 (72.3)	0.159
Female	7 (15.6)	13 (27.7)	
Risk factors			
HBV	13 (28.9)	15 (31.9)	0.753
HCV	30 (66.7)	28 (59.6)	0.481
Alcohol intake	0 (0)	3 (6.4)	0.242*
Clinical and laboratory data			
Duration of symptoms (months); median (IQR)	14 (8.5.-17.5)	12 (8–18)	0.503#
HTN	28 (62.2)	28 (59.6)	0.795
DM	27 (60)	29 (61.7)	0.867
BMI (kg/m^2), mean ± SD	33.7 (± 4)	32.5 (± 4.5)	0.181**
Elevated α-fetoprotein level	18 (40)	24 (51.1)	0.287
Elevated alanine transaminase (ALT) level	13 (28.9)	25 (53.2)	0.018
Elevated aspartate transaminase (AST) level	11 (24.4)	23 (48.9)	0.015

Chi-square test (unless otherwise mentioned) is used to determine the difference between steatotic and non-steatotic groups as regards clinical data

*Fisher's exact test

**Independent sample t test

#Mann–Whitney U test

Table 4 Comparison between positive and negative hepatic steatosis patients according to the presence of LI-RADS major and ancillary features

Characteristics		Total	Hepatic steatosis		*p* value
			Positive	Negative	
Major HCC features					
Non-rim APHE	Early	48 (52.2%)	14 (31.1%)	34 (72.3%)	0.000
	Late	44 (47.8%)	31 (68.9%)	13 (27.7%)	
Non-peripheral "washout"	No	5 (5.4%)	4 (8.9%)	1 (2.1%)	0.175
	Portal	42 (45.7%)	17 (37.8%)	25 (53.2%)	
	Delayed	45 (48.9%)	24 (53.3%)	21 (44.7%)	
Enhancing capsule	51 (55.4%)	17 (37.8%)	34 (72.3%)	0.001	
Size (mm)	< 50	62 (67.4%)	37 (82.2%)	25 (53.2%)	0.003
	50 or more	30 (32.6%)	8 (17.8%)	22 (46.8%)	
Threshold growth	17 (18.5%)	11 (24.4%)	6 (12.8%)	0.149	
Ancillary features favoring malignancy					
Corona enhancement		8 (8.7%)	3 (6.7%)	5 (10.6%)	0.714
Threshold growth		14 (15.2%)	10 (22.2%)	4 (8.5%)	0.067
Mild–moderate T2 hyperintensity		74 (80.4%)	32 (71.1%)	42 (89.4%)	0.027
Restricted diffusion		70 (76.1%)	34 (75.6%)	36 (76.6%)	0.907
Fat sparing in solid mass		5 (5.4%)	5 (11.1%)	0 (0%)	0.025
Ancillary features favoring HCC					
Non-enhancing "capsule"		7 (7.6%)	7 (15.6%)	0 (0%)	0.005
Nodule-in-nodule architecture		6 (6.5%)	2 (4.4%)	4 (8.5%)	0.677
Mosaic architecture		9 (9.8%)	3 (6.7%)	6 (12.8%)	0.486
Fat in mass, more than adjacent liver		31 (33.7%)	7 (15.6%)	24 (51.1%)	0.000
Blood products in mass		6 (6.5%)	1 (2.2%)	5 (10.6%)	0.204

steatosis 17 HCC (37.8%) displayed enhancing capsule (Figs. 3 and 4), compared to 34 HCC (72.3%) in negative hepatic steatosis patients. The result was statistically significant with *P* value 0.001.

The mean size of HCC was 52.8 ± 53.9 mm. In patients with positive hepatic steatosis, the size ranged from 11 to 200 mm (Mean 42.2 ± 51.8 mm). In patients with negative hepatic steatosis, the size ranged from 13 to 205 (Mean 62.9 ± 54.5 mm).

The threshold growth feature was observed in 17 HCC (18.5%). In the patients with positive hepatic steatosis 11 HCC (24.4%) displayed threshold growth, compared to 6 HCC (12.8%) in negative hepatic steatosis patients. The result was not statistically significant with *P* value 0.149.

As concluded, hepatic steatosis had a significant association with absent enhancing capsule, late arterial enhancement, as well as a lesion size > 50 mm.

Comparison between positive and negative hepatic steatosis patients according to the presence of ancillary features favoring malignancy (Table 4):

Fat sparing in solid mass ancillary feature had a significant association with hepatic steatosis, while "mild–moderate T2 hyperintensity" ancillary feature (Figs. 3, 5 and 6) had a significant association with absent hepatic steatosis.

Comparison between positive and negative hepatic steatosis patients according to the presence of ancillary features favoring HCC (Table 4):

"Non-enhancing capsule" ancillary feature (Fig. 5) had a significant association with hepatic steatosis, while "fat in mass, more than adjacent liver" ancillary feature had a significant association with absent hepatic steatosis.

Correlation of steatosis degree with LI-RADS major and ancillary HCC features (Table 5):

A positive relationship was found between "enhancing capsule," "lesion's size," "mild–moderate T2 hyperintensity" and "restricted diffusion" features with increased hepatic steatosis grade.

Comparison between positive and negative hepatic steatosis patients according to the presence of liver cirrhosis (Table 6):

All of the patients had signs and symptoms of liver cirrhosis.

Comparison between positive and negative hepatic steatosis patients according to the presence of portal venous thrombosis:

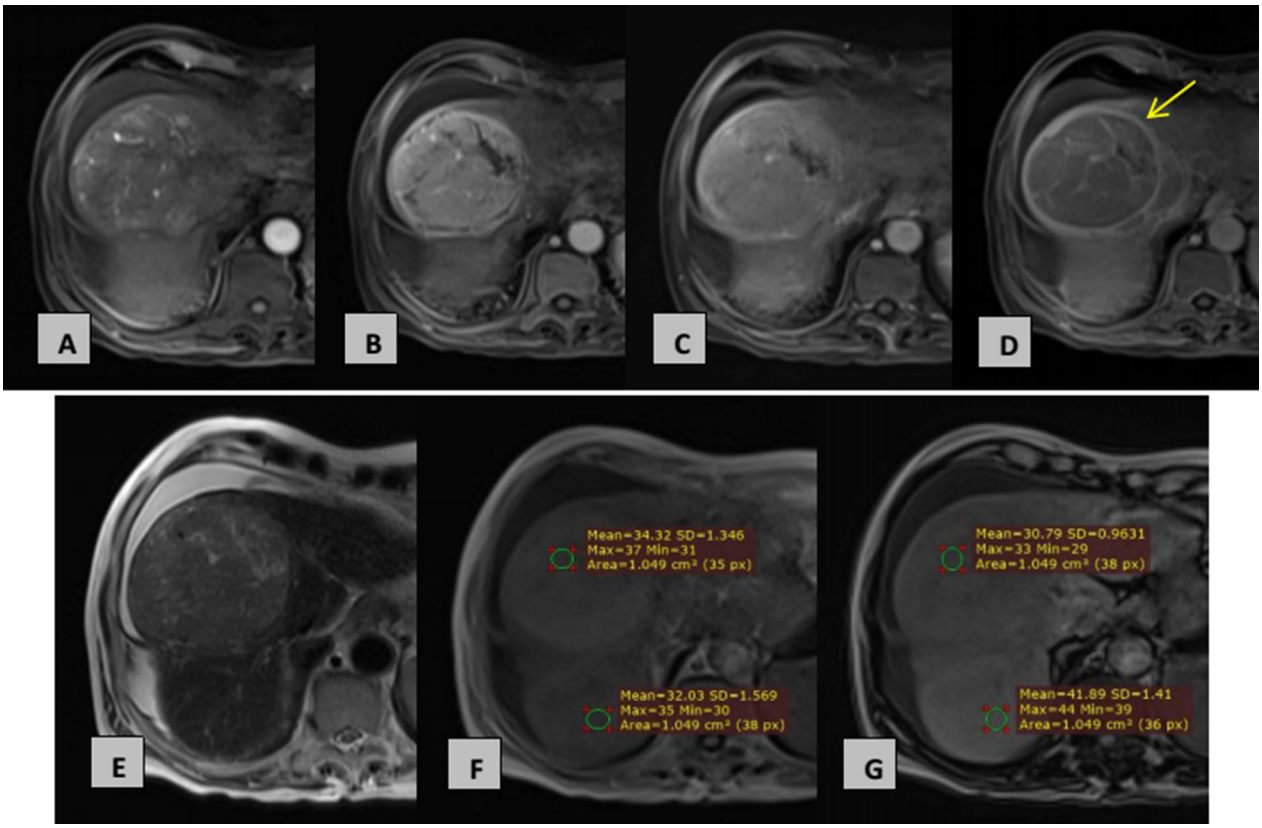

Fig. 2 A 70-year-old male patient with moderate cirrhosis and a single HCC lesion in segments IV and VIII of his liver. **A** Early arterial phase, **B** late arterial phase, **C** portal phase, **D** delayed phase **E** T2WI, **F** in-phase gradient echo, **G** opposed phase gradient echo. The lesion elicits moderate high T2 signals and shows early non-rim APHE and non-peripheral contrast washout. Mild amount of ascites is present. Hepatic fat fraction: 0% (no steatosis). Major HCC features: non-rim APHE (early), non-peripheral "washout," size = 8 × 8.8 cm and delayed enhancing capsule can be seen "arrow" in this patient (non-steatotic group)

Portal vein thrombosis was found with 27 HCC (29.3%). In the patients with positive hepatic steatosis, portal vein thrombosis was found with 12 HCC (26.7%), compared to 15 HCC (31.9%) in negative hepatic steatosis patients. The result was not statistically significant with *P* value 0.581.

Interobserver agreement

The interobserver agreement was evaluated using Cohen's kappa coefficient (Table 7). Cohen suggested the Kappa result be interpreted as follows: values ≤ 0 as indicating no agreement and 0.01–0.20 as none to slight, 0.21–0.40 as fair, 0.41–0.60 as moderate, 0.61–0.80 as substantial, and 0.81–1.00 as almost perfect agreement.

Discussion

The most common type of primary malignant tumor of the liver is HCC. Small HCC in a nodular liver is difficult to detect and characterize in sometimes. According to established recommendations and criteria, hepatocellular carcinomas are identified at cross-sectional imaging by APHE and washout in the portal venous or delayed phases. Although APHE is apparent against a low density steatotic liver, washout can be harder to identify. Fat suppression post-contrast sequences on MR imaging can cause similar problems. It is consequently critical to recognize fatty changes in the hepatic parenchyma in precontrast images. In some circumstances, image subtraction could be beneficial. As a result, standard HCC diagnostic guidelines may not be appropriate in a fatty liver [11].

Though NAFLD-associated HCC, which might be considered as another etiology of chronic hepatic disease, was not studied in this research, the presence of fatty liver might impact the HCC contrast washout irrespective of the etiology of chronic hepatic disease [12]. To determine if NAFLD impacts the accuracy of noninvasive image-based diagnosis of HCC, more studies with more patients are required.

Another factor to consider is that ultrasound is usually used as the first modality used for surveillance in individuals at high risk of HCC. Obesity frequently hinders

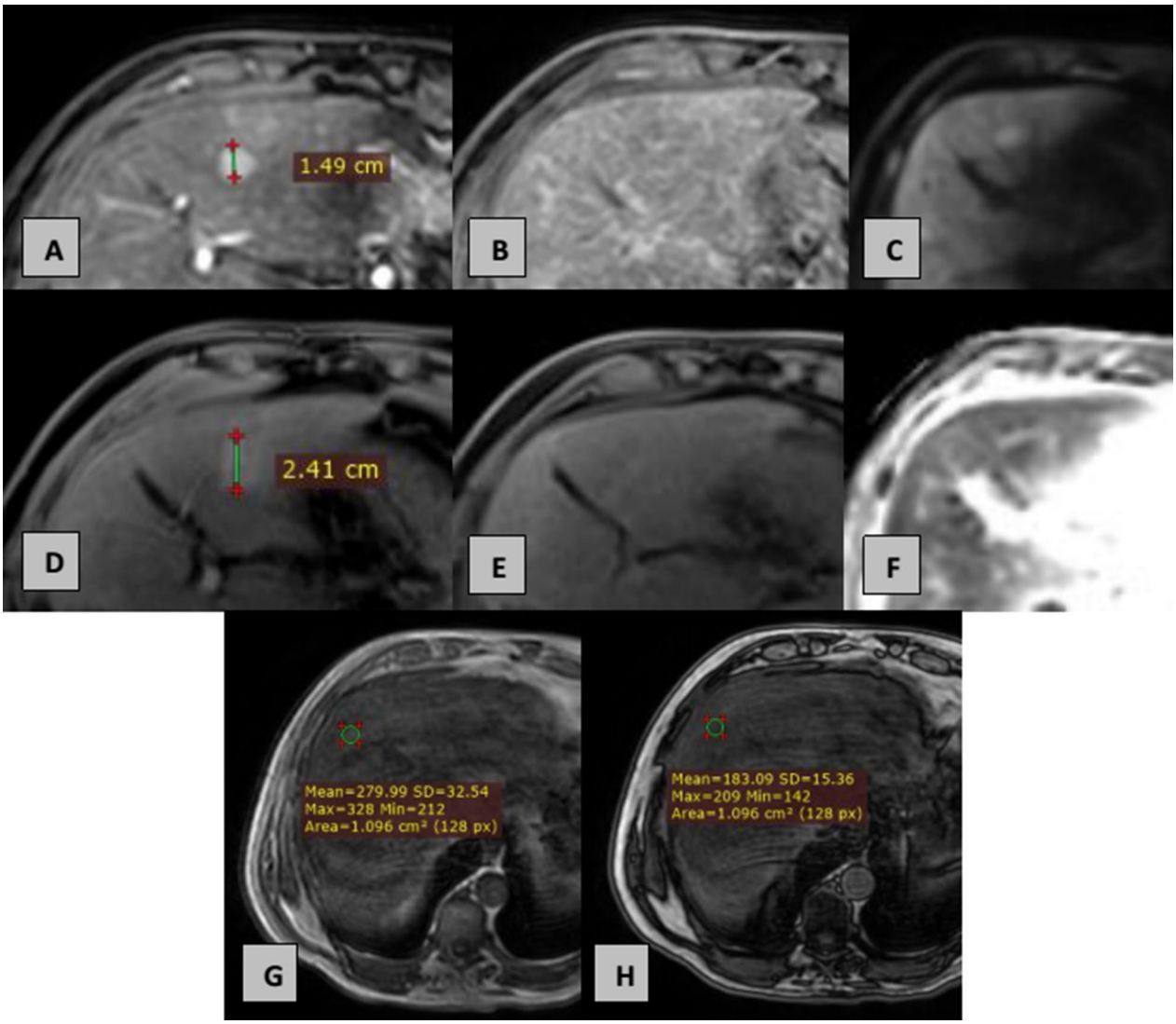

Fig. 3 A 64-year-old male patient with moderate cirrhosis and multiple HCC lesions. **A** Late arterial; **B** delayed phase; **C** diffusion-weighted images, showing a small focal lesion (HCC) at the left lobe segment II with early non-rim APHE and restricted diffusion. **D** Late arterial, **E** delayed phase, **F** ADC image obtained 3 months later showing enlargement of the lesion. **G** In-phase gradient echo, **H** opposed phase gradient echo images showing Hepatic fat fraction: 17.2% (moderate steatosis). Major HCC features: Non-rim APHE (late) "Please note the absence of the delayed enhancing capsule in this case." Ancillary HCC features favoring malignancy: restricted diffusion, subthreshold growth "Unequivocal size increase of a mass, less than threshold growth"

the thoroughness of ultrasonography examinations in patients with hepatic steatosis. According to del Poggio et al. [13], a BMI of more than 25 leads to a failure of US test of the liver, so computed tomography or magnetic resonance imaging are frequently performed to investigate the liver. Our research could be beneficial since it depicts the MRI features of HCC in patients with hepatic steatosis.

In our study that included 92 patients, we found that HCC in steatotic liver appeared as a hepatic focal lesion with arterial hyperenhancement. Most notably, we reported that 28 (62.2%) HCC in patients having hepatic steatosis might not show the "enhancing capsule" feature. Previous studies have linked a lack of contrast washout or enhancing tumoral capsule on MRI to a higher grade of hepatic fat deposition in individuals with NAFLD [12].

The mean greatest dimension of HCC nodules in fatty liver group was 42.2 ± 51.8 mm, while the mean largest diameter of HCC nodules in non-fatty liver group was 62.9 ± 54.5 mm. Min et al. [12] observed a median diameter of HCC of 30 mm in both fatty and non-fatty liver groups in their research of 566 individuals.

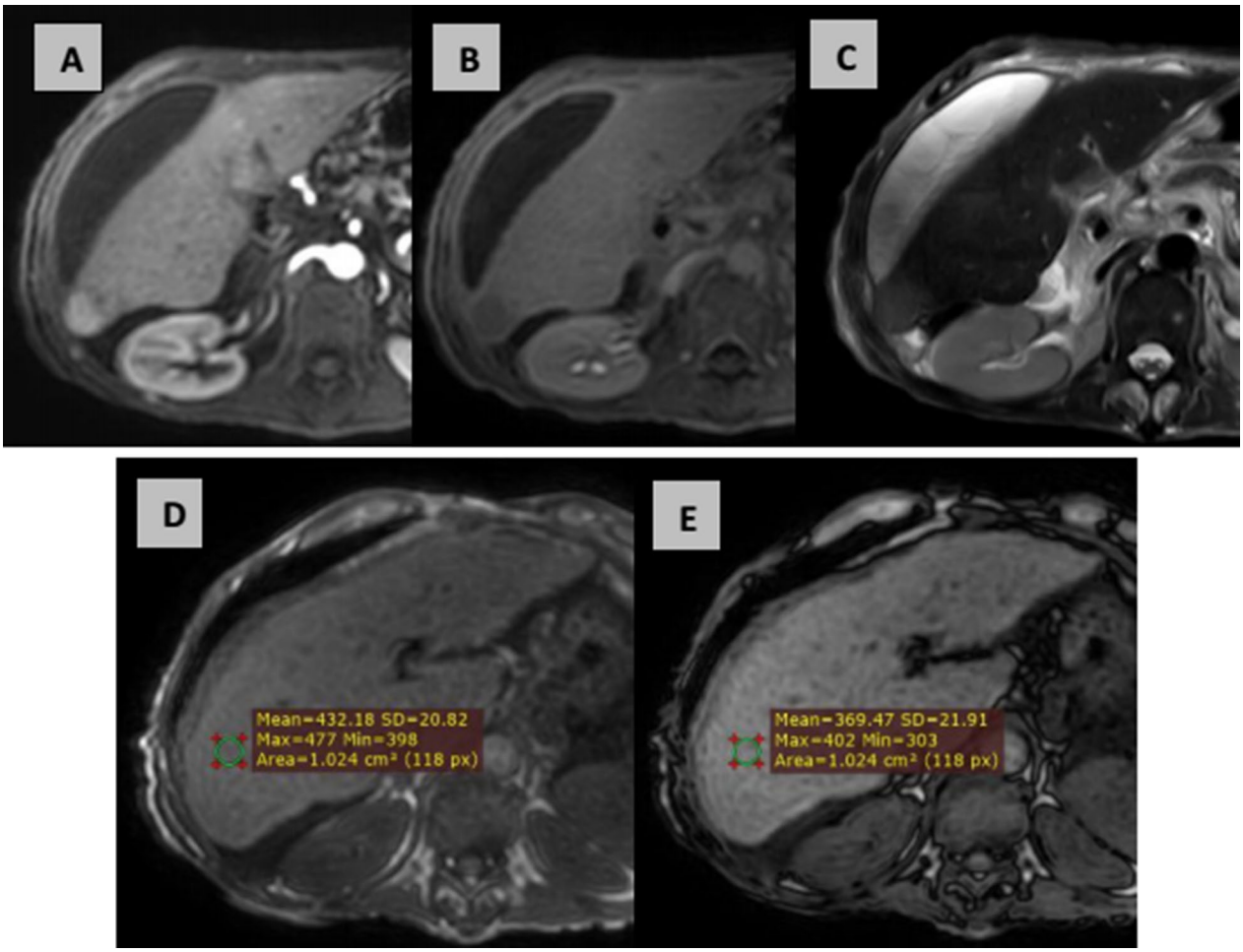

Fig. 4 A 59-year-old male patient with moderate cirrhosis and single HCC lesion at segment VI. **A** Early arterial phase, **B** delayed phase, **C** T2 WI, **D** in-phase gradient echo, **E** opposed phase gradient echo. The lesion elicits mild high T2 signals and shows early non-rim APHE and non-peripheral contrast washout. Moderate amount of ascites is present. Hepatic fat fraction: 7.3% (mild steatosis). Major HCC features: non-rim APHE (early), non-peripheral "washout" (early) and size = 2.3 × 2.5 cm. Ancillary HCC features favoring malignancy: mild T2 hyperintensity. Please note the absence of the delayed enhancing capsule in this case

In the current study, all HCC (92/92; 100%) showed APHE. All HCC (100%) showed hyperenhancement in the research by Al-sharhan et al. [7], which comprised 30 patients with non-alcoholic steatohepatitis (NASH). In Thompson et al. [5], research of 48 individuals with NAFLD and APHE was seen in 45 of the 48 participants (93%). Hypervascular nodules were seen in all 16 patients in Iannaccone et al. [14] investigation which comprised 16 individuals with NAFLD (100%). However, these studies included patients with NAFLD/NASH and not just those with hepatic steatosis.

The fatty liver group had significantly higher rate of late APHE compared to the non-hepatic steatosis group, late APHE was observed in 31 HCC (31/45; 68.9%) in the hepatic steatosis group patients, and in the non-fatty liver group late APHE was found in 13 HCC (13/47; 27.7%).

In our research, we discovered that 4 HCC (8.9%) in patients with hepatic steatosis did not exhibit the "washout" feature in the portal venous or delayed phases of the study, compared to one (2.1%) in the non-fatty liver group. This was in consistent with the results revealed by Min et al. [12], where the rates of absence of washout appearance on MRI were similar in the fatty liver and non-fatty liver groups (22.9% [28/122] vs. 25.6% [92/360], $p = 0.565$), whereas in the CT studies a significant difference was found between both groups. Iannaccone et al. [14] revealed absent contrast washout in only 2/16 HCC (13%) in patients with NAFLD. Of interest, in the research by Thompson et al. [5] that involved 48 individuals with NAFLD, HCC showed contrast washout in 38/48 patients (79%). In the study by Al-sharhan et al. [7], 12/30 HCC nodules (40%) in patients with NASH did not show the "washout" feature.

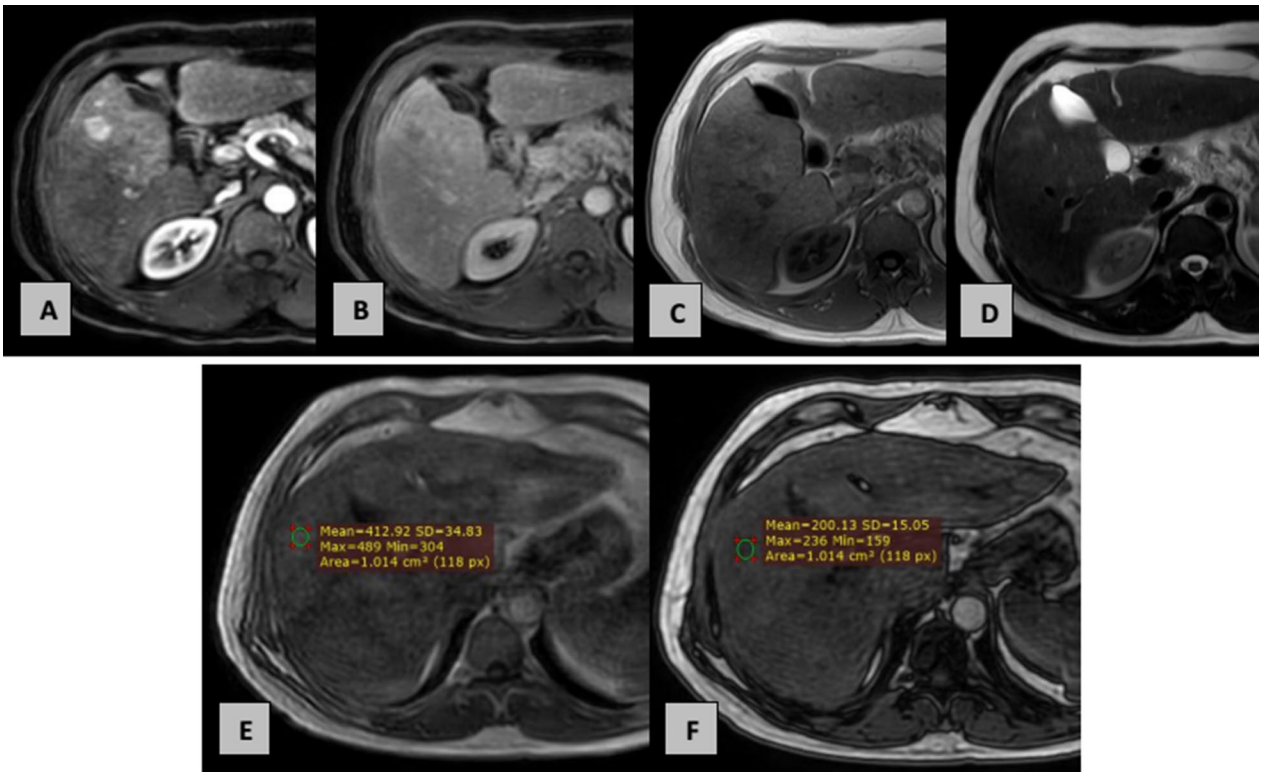

Fig. 5 A 54-year-old male patient with mild cirrhosis and single HCC at segment V. **A** Late arterial phase, **B** delayed phase, **C** T1 WI, **D** T2 WI, **E** in-phase gradient echo, **F** opposed phase gradient echo. The lesion elicits low T1 and mild high T2 signals and shows non-rim APHE and non-peripheral contrast washout. Hepatic fat fraction: 25.7% (moderate steatosis). Major HCC features: non-rim APHE (late), non-peripheral "washout" (late) and size = 2 × 2.2 cm. Ancillary HCC features favoring malignancy: mild T2 hyperintensity. Ancillary features favoring HCC in particular: non-enhancing capsule. The hepatic fat fraction in this case was measured at segment V instead of segment VII to avoid the areas of artifact

In our study, the hepatic steatosis group had significantly lower rate of enhancing tumor capsule compared with the non-hepatic steatosis group, enhancing capsule was observed in 17 HCC (17/45; 37.8%) in the hepatic steatosis group patients, in the non-hepatic steatosis group enhancing capsule was found in 34 HCC (34/47; 72.3%). In the study by Al-sharhan et al. [7], enhancing capsule was found in 18 HCC (18/30; 60%) in patient underwent MRI. Similar findings were revealed by Iannaccone et al. [14] who reported enhancing tumor capsule in 15/22 HCC (68%) in patients with NAFLD. In the study by Thompson et al. [5], HCC showed encapsulation in 34/48 patients (71%) with NAFLD. Tumor capsule was found in 43/103 HCC (41.7%) in the Rimola et al. [15] research, in which no patients had NASH, and was a highly specific.

Feature of HCC (96.5% specificity). It is obvious that the frequency of tumor capsule in HCC varies significantly between studies, depending on ethnicity and the type of the underlying illness.

In the current research, a higher proportion of HCCs displayed high T2W signal in patients with no hepatic steatosis; 42 HCC (42/47; 89.4%), compared to 32 HCC (32/45; 71.1%) in hepatic steatosis patients. In the research by Thompson et al. [5], the majority of HCCs (88%) in NAFLD patients were T2W hyperintense. Our findings, on the other hand, diverge with those of Iannaccone et al. [13], where all tumors 22/22 HCC (100%) in NAFLD patients were T2 hyperintense.

It was also found that the hepatic steatosis group had significantly higher rate of "fat sparing in solid mass" feature compared to non-hepatic steatosis group, fat sparing was observed in 5 HCC (5/45; 11.1%) in the hepatic steatosis group patients, while in the non-hepatic steatosis group no HCCs 0 (0%) showed fat sparing.

Also, intratumoral fat was displayed in 7 HCC (7/45; 15.6%) in the fatty liver group, with a significant difference in comparison to the non-fatty liver group where 24 HCC (24/47; 51.1%) showed intralesional fat. In the study by Al-sharhan et al. [7], intratumoral fat was found in 11/21 HCC (52%) in patients with NASH. In the research done by Rimola et al. [15], intratumoral fat was detected in 43/103 HCC (41.7%) in a population of liver cirrhosis patients and no NASH.

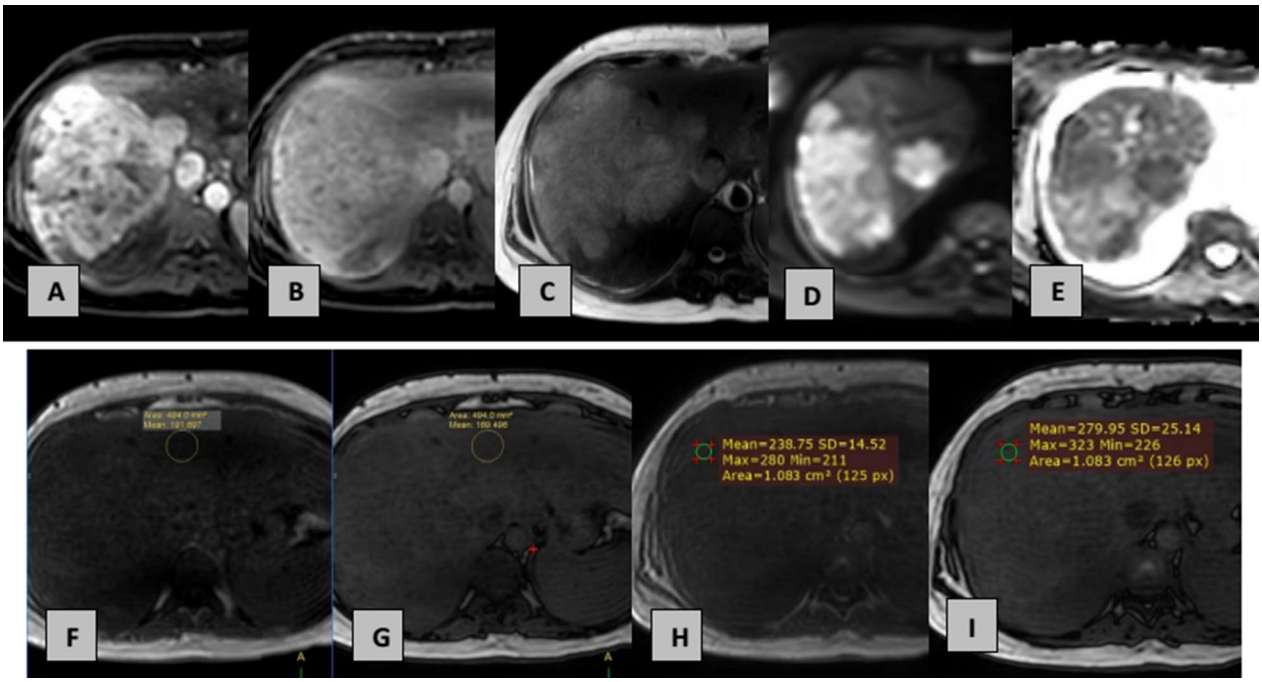

Fig. 6 A 40-year-old male patient with moderate cirrhosis and a single HCC lesion in segments VIII, VII, V, and IV. **A** Early arterial phase, **B** delayed phase **C** T2WI, **D** diffusion WI **E** ADC map, **F** in-phase gradient echo, **G** opposed phase gradient echo **H** in-phase gradient echo measuring the fat fraction within the lesion, **I** opposed phase gradient echo measuring the fat fraction within the lesion.The lesion elicits moderate high T2 signals with restricted diffusion and shows early non-rim APHE and non-peripheral contrast washout. Hepatic fat fraction: 5.8% (Mild steatosis). Major HCC features: non-rim APHE (early), non-peripheral "washout" (late) and size = 13.5 × 14.5 cm. Ancillary HCC features favoring malignancy: Moderate T2 hyperintensity, restricted diffusion and fat sparing in solid mass "Relative paucity of fat in solid mass relative to steatotic liver": (fat fraction in the lesion = 0%)

Table 5 Correlation of steatosis degree with LI-RADS major and ancillary HCC features

	Steatosis grade		Hepatic fat fraction %	
	r	*P**	*r*	*P**
Major HCC features				
Non-peripheral "washout"	− 0.169	0.268	− 0.186	0.220
Enhancing "capsule"	− 0.441	0.002	− 0.219	0.149
Size (mm)	− 0.331	0.026	− 0.264	0.080
Threshold growth	− 0.093	0.543	0.072	0.640
Ancillary features favoring malignancy				
Corona enhancement	− 0.151	0.322	− 0.206	0.175
Subthreshold growth	0.052	0.733	− 0.012	0.936
Mild–moderate T2 hyperintensity	− 0.454	0.002	− 0.370	0.012
Restricted diffusion	− 0.308	0.039	− 0.327	0.029
Fat sparing in solid mass	0.153	0.317	0.060	0.696
Ancillary features favoring HCC				
Non-enhancing "capsule"	0.164	0.282	0.038	0.805
Nodule-in-nodule architecture	− 0.122	0.425	− 0.008	0.957
Mosaic architecture	− 0.151	0.322	0.021	0.893
Fat in mass, more than adjacent liver	− 0.107	0.483	− 0.033	0.829
Blood products in mass	− 0.085	0.578	0.093	0.544

r Spearman correlation coefficient

*Spearman correlation test

Table 6 Comparison between positive and negative hepatic steatosis patients according to presence liver cirrhosis

Characteristics	Total	Hepatic steatosis		*p* value
		Positive	Negative	
Liver cirrhosis				
Mild	31 (33.7%)	14 (31.1%)	17 (36.2%)	0.189
Moderate	36 (39.1%)	19 (42.2%)	17 (36.2%)	
Severe	25 (27.2%)	12 (26.7%)	13 (27.7%)	

In the current study, a higher proportion of HCCs showed non-enhancing capsule in patients with hepatic steatosis; 7 HCC (7/45; 15.6%), while in the non-hepatic steatosis group no HCCs 0 (0%) showed non-enhancing capsule.

As regards the impact of the degree of fatty liver on the major and ancillary HCC features, the "enhancing capsule," "mild–moderate T2 hyperintensity," and "restricted DWI" features are less commonly seen in cases of moderate to severe hepatic steatosis than in those of mild hepatic steatosis. Our study also showed that HCCs tends to be of a smaller size as the hepatic steatosis degree increased.

Table 7 Interobserver agreement for HCC features in positive and negative hepatic steatosis patients

	Non-fatty liver		Fatty liver	
	IOA percent (%)	Kappa	IOA percent (%)	Kappa
APHE (early)	100	1	100	1
APHE (late)	100	1	100	1
Non-peripheral "washout" (portal)	97.9	0.957	95.6	0.908
Non-peripheral "washout" (delayed)	97.9	0.957	95.6	0.910
Enhancing capsule	93.6	0.827	93.3	0.862
Size (50 mm)	100	1	100	1
Threshold growth	95.7	0.832	97.8	0.942
Corona enhancement	95.7	0.810	88.9	0.483
Subthreshold growth	100	1	100	1
Mild–moderate T2 hyperintensity	100	1	97.7	0.944
Restricted diffusion	95.7	0.873	93.3	1
Fat sparing in solid mass		…	100	1
Non-enhancing "capsule"-		…	97.8	0.920
Nodule-in-nodule architecture	100	1	100	1
Mosaic architecture	97.9	0.911	97.8	0.845
Fat in mass, more than adjacent liver	97.9	0.957	97.8	0.920
Blood products in mass	95.7	0.810	95.6	0.483

The study has some limitations. Of these, two main limitations are the retrospective aspect of the study, which leads to inclusion bias, as well as the small number of study population. Furthermore, to quantify hepatic steatosis, the hepatic FS % was utilized, and there are known limitations to this method. However, because the ratio of fat fraction rather than absolute fat measurement is used, hepatic FS percent is less susceptible to changes in MRI technique over time. Furthermore, we did not undergo a comprehensive imaging–pathologic correlation to identify MRI characteristics associated with tumor grade and the effect of tumor fat fraction on MRI signal intensity fluctuation on Dixon images. Lastly, further prospective investigations are necessary to assess the true efficacy of MRI as a screening modality in individuals with hepatic steatosis.

Conclusions

As regards to the major HCC features, we concluded that hepatic steatosis had a significant association with absent enhancing capsule, late arterial enhancement, as well as a lesion size less than 50 mm. As regards to the ancillary HCC features, we concluded that "Fat sparing in solid mass" and "non-enhancing capsule" ancillary features had a significant association with hepatic steatosis, while "mild–moderate T2 hyperintensity" and "fat in mass, more than adjacent liver" ancillary features had a significant association with absent hepatic steatosis. In conclusion, the findings of our retrospective study are coincide with a recent retrospective studies demonstrated that "enhancing capsule" feature of HCC was less frequently observed in patients with hepatic steatosis compared to non-hepatic steatosis patients. In our study, we have compared the MRI features of HCC in patients with hepatic steatosis to those in patients without hepatic steatosis. Our findings imply that existing imaging criteria for the noninvasive characterization of HCC in individuals with hepatic steatosis should be utilized with care.

Abbreviations

AFLD	Alcoholic fatty liver disease
APHE	Arterial phase hyperenhancement
BMI	Body mass index
CT	Computed tomography
DWI	Diffusion-weighted image
FS	Fat signal
HCC	Hepatocellular carcinoma
LI-RADS	Liver Imaging Reporting and Data System
MRI	Magnetic resonance imaging
NAFLD	Non-alcoholic fatty liver disease
NASH	Non-alcoholic steatohepatitis
PACS	Picture archiving and communication system
PHTN	Portal hypertension
ROI	Region of interest
TSE	Turbo spin echo
SIP	Signal in phase
SOP	Signal out of phase
SSH-TSE	Single-shot turbo spin echo
UFSE	Ultra-fast spin echo

Acknowledgements
Not applicable.

Author contributions
MFO contributed to participation in the study design. MRI was involved in assessment and manuscript editing. ARM contributed to patients collection and clinical assessment. AAG was involved in shared in statistical analysis, data collection, and MRI assessment. MMA contributed to put the idea of the study, performed the statistical analysis, and participated in the study design. BEM was involved in participation in the study design. MRI contributed to assessment and manuscript editing. All authors have read and approved the final manuscript.

Funding
Not applicable (no funding received for this study).

Availability of data and materials
All the datasets used and analyzed in this study are available with the corresponding author on reasonable request.

Declarations

Ethics approval and consent to participate
The study was approved by the research committee of faculty of medicine, Kasr Alainy hospital. Cairo University November 2019. No reference number provided.

Consent for publication
The institutional review board waived the necessity for written informed consent because of the retrospective methodology.

Competing interests
The authors declare that they have no competing interests.

Received: 6 September 2022 Accepted: 1 February 2023
Published online: 09 February 2023

References

1. Okushin K, Casuccio A, Zafonte R, et al (2018) Advances in fatty liver disease. Adv Fatty Liver Dis 331.
2. Hayashi T, Saitoh S, Takahashi J et al (2017) Hepatic fat quantification using the two-point Dixon method and fat color maps based on non-alcoholic fatty liver disease activity score. Hepatol Res 47(5):455–464
3. Pierre TG, House MJ, Bangma SJ et al (2016) Stereological analysis of liver biopsy histology sections as a reference standard for validating non-invasive liver fat fraction measurements by MRI. PLoS ONE 11(8):e0160789
4. El-Said N, Kaddah R, Abel-Fattah M et al (2016) Subtraction MRI versus diffusion weighted imaging: which is more accurate in assessment of hepatocellular carcinoma after trans arterial chemoembolization (TACE)? Egypt J Radiol Nucl Med 47(4):1251–1264
5. Thompson SM, Garg I, Ehman EC et al (2018) Non-alcoholic fatty liver disease-associated hepatocellular carcinoma: effect of hepatic steatosis on major hepatocellular carcinoma features at MRI. Br J Radiol 91(1092):20180345
6. Ronot M, Vilgrain V (2014) Hepatocellular carcinoma: diagnostic criteria by imaging techniques. Best Pract Res Clin Gastroenterol 28(5):795–812
7. Al-Sharhan F, Dohan A, Barat M et al (2019) MRI presentation of hepatocellular carcinoma in non-alcoholic steatohepatitis (NASH). Eur J Radiol 119:108648
8. Mitchell DG, Bruix J, Sherman M et al (2015) LI-RADS (Liver Imaging Reporting and Data System): summary, discussion, and consensus of the LI-RADS Management Working Group and future directions. Hepatology 61(3):1056–1065
9. Ma X, Holalkere NS, Mino-Kenudson M et al (2009) Imaging-based quantification of hepatic fat: methods and clinical applications. Radiographics 29(5):1253–1277
10. Venkatesh SK, Hennedige T et al (2017) Imaging patterns and focal lesions in fatty liver: a pictorial review. Abdom Radiol 42(5):1374–1392
11. Venkatesh SK, Hennedige T, Johnson GB et al (2017) Imaging patterns and focal lesions in fatty liver: a pictorial review. Abdom Radiol 42:1374–1392
12. Min JH, Kang TW, Kim YY et al (2021) Vanishing washout of hepatocellular carcinoma according to the presence of hepatic steatosis: diagnostic performance of CT and MRI. Eur Radiol 31:3315–3325
13. Del Poggio P, Olmi S, Ciccarese F et al (2014) Factors that affect efficacy of ultrasound surveillance for early stage hepatocellular carcinoma in patients with cirrhosis. Clin Gastroenterol Hepatol 12(11):1927–1933
14. Iannaccone R, Piacentini F, Murakami T et al (2007) Hepatocellular carcinoma in patients with nonalcoholic fatty liver disease: helical CT and MR imaging findings with clinical-pathologic comparison. Radiology 243(2):422–430
15. Rimola J, Forner A, Tremosini S et al (2012) Non-invasive diagnosis of hepatocellular carcinoma $\leq$ 2 cm in cirrhosis. Diagnostic accuracy assessing fat, capsule and signal intensity at dynamic MRI. J Hepatol 56(6):1317–1323

Publisher's Note